

# PET with $^{18}\text{F}$ -Fluoride: Effects of Iterative versus Filtered Backprojection Reconstruction on Kinetic Modeling

Christiaan Schiepers, Johan Nuyts\*, Hsiao-Ming Wu, *Member, IEEE*, Ramesh C. Verma  
 Olive View-UCLA Medical Center, Los Angeles-Sylmar, California  
 University of Leuven, KU Leuven, Belgium\*

## *Abstract*

High focal uptake in patients poses particular problems in PET imaging. Filtered backprojection (FBP) introduces disturbing streak artifacts, adversely affecting the identification of structures and delineation of regions. Iterative reconstruction methods (MLEM) provide images of superb quality, however, the accuracy of quantitative results obtained from MLEM images has not been established for clinical data.

Dynamic images were acquired over 1 hr with PET and  $^{18}\text{F}$ -fluoride in 6 patients with an old unilateral hip fracture. FBP and MLEM reconstruction was performed. Since the bladder was in the FOV and filled up with fluoride, FBP produced streaks hampering region delineation. Bone blood flow ( $k_1$ ) and fluoride influx rate ( $K_i$ ) were estimated with a 3 compartment model. Analyzed regions ( $n=190$ ) showed correlation coefficients between FBP and MLEM: 0.88 for  $k_1$  and 0.97 for  $K_i$ . Affected and normal femoral head regions ( $n=30$ ) yielded  $r=0.89$  for  $k_1$  and  $r=0.95$  for  $K_i$ . Variations up to 46% were seen in individual data.

**Conclusion:** in patients MLEM provides superior images at the expense of an increased reconstruction duration. Our procedure appeared acceptable in clinical routine. Quantitative estimates obtained with kinetic modeling from MLEM data were reliable and correlated highly to those obtained with the standard, validated FBP algorithm.

## I. INTRODUCTION

In dynamic PET imaging, organs with high uptake pose particular problems. In reconstructing areas of high activity, the standard filtered back projection (FBP) algorithm produces disturbing streak artifacts obscuring nearby located organs with lower activity (see Figure 1). Thus, the identification of anatomical structures and delineation of regions of interests (ROIs) is adversely affected. ROIs are drawn around the structures to be investigated and time activity curves (TACs) are generated that are used for further analysis or quantitation. Iterative reconstruction methods provide images of superb quality (see Figure 1), but stopping criteria are ill-defined, too many iterations produce noisy 'unrealistic' images, and the resolution in the final reconstructed image is spatially variant and position dependent [1]. Moreover, the obtained spatial resolution is not a function of the number of iterations and cannot be predicted [2]. Therefore, we set out to compare the effects of two reconstruction techniques on the final quantitative results: the standard FBP vs. the iterative MLEM (maximum likelihood expectation maximization). Since we are interested in a procedure that suits the clinical routine, only 1 set of final images is reconstructed. Subsequently, the data of the obtained TACs were fitted with a 3 compartment

model that is used to estimate the value of physiologic variables such as tracer flow ( $\text{ml}/\text{min}/\text{ml}$ ) and influx rate ( $\text{ml}/\text{min}/\text{ml}$ ) into the organ under investigation.

## II. METHODS

### *Acquisition*

Dynamic images were acquired over 1 hr with a commercial PET system (Siemens-CTI ECAT-931) and  $^{18}\text{F}$ -fluoride as radiopharmaceutical. Attenuation correction was performed with a transmission scan of 15 minutes duration. In 6 patients with an old unilateral hip fracture, imaging of the pelvis and both hips was performed. Since the bladder is in the field of view and fills up with fluoride, an extremely hot organ is present in the last part of the study.

### *Standard reconstruction*

A standard filtered backprojection algorithm was used, which was available on the commercial system. FBP was performed with a ramp filter and Hanning window with the cut-off at 0.35 of the Nyquist frequency, i.e. sampling frequency of  $0.32 \text{ mm}^{-1}$  and final image resolution of 9 mm FWHM.

### *Iterative reconstruction*

In our MLEM implementation, the computations are accelerated in two complementary ways: a) the number of projection/backprojection operations is reduced by making use of the ordered subsets (OS) strategy [3]; b) the number of computations executed per projection/backprojection is reduced by pre-calculating the interpolation weights [4].

In the OS strategy [3], only a subset of the projections (or sinogram-rows) is used in a subiteration. Assuming a

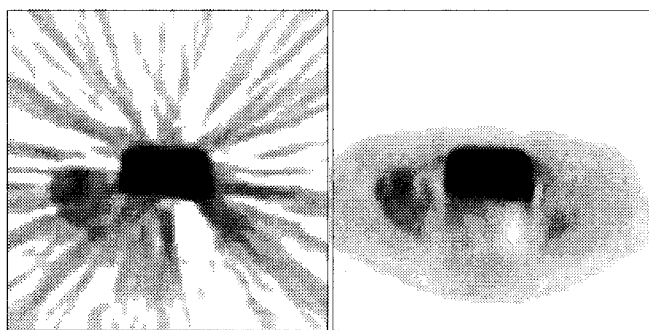


Figure 1. Reconstructions of a typical transverse plane with FBP (left panel) and OS-MLEM (right panel). Note the streak artifacts and the filled hot bladder.

sinogram of R rows, with S of these used in a subset, the number of computations in the subiteration is reduced by a factor of S/R. A full OS iteration consists of R/S subiterations, so every projection is used once. For optimal performance, the projections in the same subset should be uniformly spread over 180 degrees, i.e. equidistant sampling of the S projections of the subset. In addition, the angular distance between subsequent subsets should be as large as possible, to maximize the amount of information added by every subiteration. For noisy data, each subset directs the reconstruction towards different solutions. As a result, the reconstruction image oscillates between the different solutions at higher iteration numbers. The number of subsets must be decreased to approach the ML solution. Therefore, we use a set of iterations with decreasing number of subsets, and end with a few complete ML-iterations.

In order to reduce the storage requirements for the pre-calculated interpolation coefficients [4], the sinograms are resampled to an intermediate format in which the interpolation coefficients for parallel lines are identical. The number of coefficients is then proportional to b x N x R, where the dimension of the reconstruction image equals N x N, the dimension of the sinogram N x R, and b is the number of bytes stored for every coefficient (pixel address and interpolation weight are stored together). The sinograms are resampled to the intermediate format prior to backprojection, and again in the original format after projection. As a result, the resampling is implemented as part of the projection/backprojection operation, which produces some smoothing. All computations involving the measured data, are performed using the original sinogram format. Detector sensitivity calibration and attenuation compensation are included in the projection/backprojection operation. The limited spatial resolution of the detectors and the contribution of randoms and scatter were ignored. The attenuation factors were derived from the ratio of smoothed blank and transmission scans.

The final set of iterations consisted of 1 main iteration with 8 subsets, followed by 4 main with 4 subsets and finally 8 main iterations with 1 subset (true MLEM). This iteration scheme was a compromise between reasonable computation time, adequate diagnostic image quality and quantitative accuracy. Empirically, we found that this sequence usually supplied high quality images. With different iteration schemes it was found that high iteration numbers (>50) decreased visual image quality, produced ringing artifacts and provided a final image result of poor diagnostic and 'non-physiologic' quality.

Both FBP and MLEM images were reconstructed in a 192x192 matrix, with a zoom of 1 amounting to a final pixel size of 3.1 mm. Reconstruction time on a SUN SPARC 10 computer for 256 projection angles was 6.6 s per iteration.

### Kinetic modeling

Regions were drawn over abnormal bone areas and mirrored to the contra-lateral control side. This was done on the MLEM images and ROIs were then transferred to the FBP images; hereafter all TACs were generated.

A 3 compartment model was utilized to analyze the data. A constrained optimization tool using a sequential quadratic programming algorithm (MATLAB) was implemented on a

Power Macintosh computer to estimate bone blood flow (k1) and fluoride influx rate (Ki) using the model of Figure 2. The k-values represent the rate constants of tracer transport. The input curve (plasma clearance of tracer) was measured with blood withdrawn from the radial artery. The output curve is the activity change in function of time of a certain ROI, i.e. integrated activity in the ECF and bone compartments plus a fraction of the input function, in the specific TAC. The influx rate Ki equals  $(k_1 \cdot k_3) / (k_2 + k_3)$ . For a detailed description of the fluoride kinetic model in humans, the reader is referred to Hawkins et al. [5].

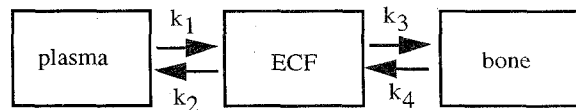


Figure 2 Three compartment kinetic model with freely diffusible  $^{18}\text{F}$ -fluoride in plasma and extra-cellular fluid (ECF), and bound  $^{18}\text{F}$ -fluoride in the bone compartment.

### III. RESULTS

FBP introduced streaks, hampering the definition of ROIs over the hips. Especially the normal hip with low uptake was difficult to see. MLEM, on the contrary, did not produce these streak artifacts and supplied high quality images on which the hip could easily be identified (see Figure 1).

Of all 190 analyzed ROIs from the 6 different patients, the results of k1 and Ki are shown in the scatter diagrams between FBP and MLEM (Figures 3 and 4). The k1 and Ki estimates obtained with TACs from the FBP method correlated well with those obtained from the MLEM method. The correlation coefficients (r) of k1 and Ki were 0.88 and 0.97, respectively. The corresponding regression lines were:

$$\begin{aligned} k1_{MLEM} &= 0.95 * k1_{FBP} && \text{(see Figure 3)} \\ Ki_{MLEM} &= 0.96 * Ki_{FBP} && \text{(see Figure 4)} \end{aligned}$$

The results for the affected and normal femoral head of the hips (n=30) yielded r=0.89, slope = 0.95 for k1 and r=0.95, slope = 0.96 for Ki. For the hip bone ROIs, variations up to 46% (relative error) between MLEM and FBP were seen in Ki. The mean difference in Ki values of the abnormal hips was 14% ( $sd = 15\%$ , n=15).

The sum of residuals of fitting ( $c$  = counts/pixel/min, and D = image duration):

$$\sum_{n=1}^{\# \text{ frames}} (c_{\text{fitted}}(n) - c_{\text{measured}}(n))^2 * D(n)$$

was smaller for MLEM than FBP: on average 0.24 vs. 0.43 and the difference was statistically significant ( $p<.001$ ).

In general, the image quality of the iterative technique was far superior. However, reconstruction time increased by a factor of 10 on a SUN SPARC-10 station with our set of main- and sub-iterations (OS) when compared to the standard FBP.

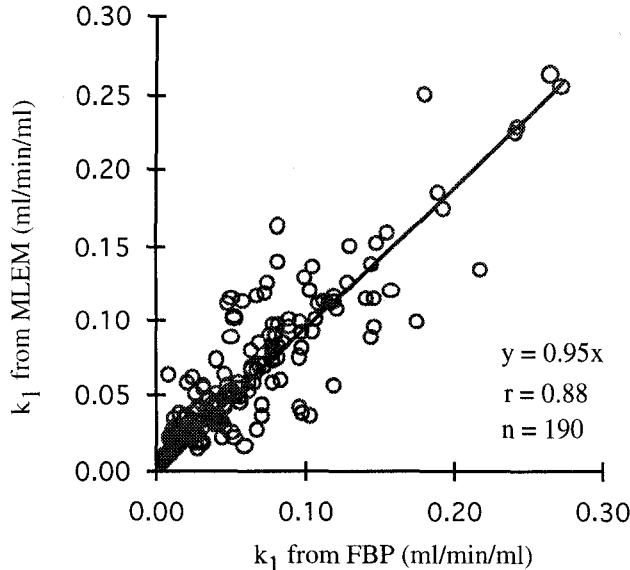


Figure 3. Scatter diagram of all 190 data points (n) for  $k_1$  or flow values of the standard FBP (x) and the iterative reconstruction (y). Corresponding regression line is also shown. r - correlation coefficient.

Our results indicate that reliable estimates can be obtained with MLEM reconstructions and that there are no statistically significant changes for  $k_1$  and  $K_i$  ( $p=NS$ , t-test). This indicates that the streak artifacts have a minor influence on the final modeling parameters. However, we arrived at these results by using ROIs drawn on high quality images (MLEM) which were subsequently transferred to the FBP images. Modeling results would have been different if the ROIs had to be drawn directly on the FBP reconstructions. In the latter case, streak artifacts would have prevented an accurate delineation of the structures involved, leading to different estimates of  $k_1$  and  $K_i$ .

The effect of the stopping criterion was not investigated here. MLEM with a limited number of iterations produced ringing. High numbers of iterations ( $>200$ ) resulted in noisy images. An empirical criterion was used, i.e. the physician considered the image quality appropriate for interpretation. It has been shown that continuation of iterations further reduces the bias, at the cost of higher noise values [6]. In addition, the final spatial resolution depends on both iteration number and position [1]. Consequently, the optimum number of iterations is different for every region and is expected to be higher for regions larger in size. Since the final image resolution is position dependent in MLEM and cannot be predicted in advance, the recovery coefficients for small ROIs are unknown.

Constraining the noise by using prior distributions is probably superior to stopping of the iterations. Good results were reported by Mumcuoglu et al. [7]. However, this requires much longer processing times, decreasing the value of this procedure in clinical routine considerably.

The attenuation coefficients were calculated in the classical way. Further improvement of image quality is expected if the attenuation factors are derived from ML or maximum-a-posteriori transmission reconstructions [7].

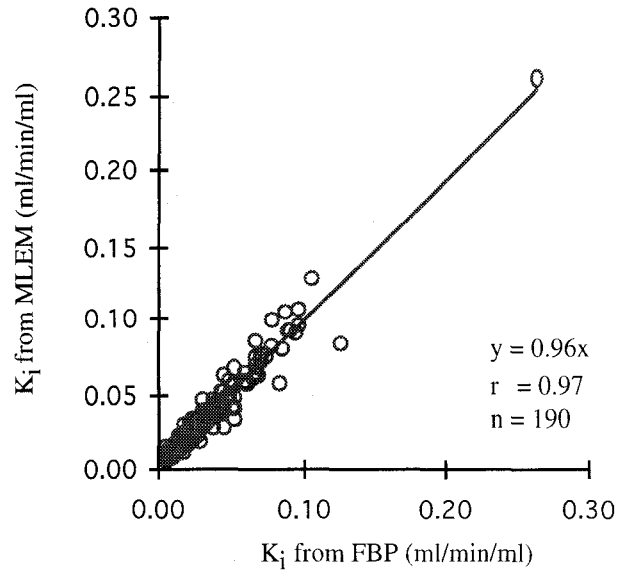


Figure 4. Scatter diagram of all 190 data points (n) of macro  $K_i$ , i.e. fluoride influx rate, for the two evaluated reconstruction techniques. Note the close correspondence and fit of the linear regression line.

#### IV. CONCLUSION

MLEM provides images of superior quality at the expense of a ten times increased reconstruction duration over FBP. Quantitative estimates of flow and influx rate, obtained with kinetic modeling on data generated with MLEM were reliable and correlated highly to those obtained with the routinely used and clinically validated FBP algorithm.

#### V. REFERENCES

- [1] J.S. Liow, S.C. Strother. "The convergence of object dependent resolution in maximum likelihood based tomographic image reconstruction. *Phys Med Biol*, 1993; 38: pp. 55-70
- [2] J. Nuyts, P. Dupont, V. Van den Maegdenbergh, S. Vleugels, P. Suetens, L. Mortelmans. "A study of the liver-heart artifact in emission tomography." *J Nucl Med*, 1995; 36: pp. 133-139
- [3] M.H. Hudson, R.S. Larkin. "Accelerated image reconstruction using ordered subsets of projection data," *IEEE Trans MI*, 1994; 13: pp. 601-609
- [4] J. Nuyts, P. Dupont, C. Schiepers, L. Mortelmans. "Efficient storage of the detection probability matrix for reconstruction in PET," *J Nucl Med*, 1994; 35: p. S187
- [5] R.A. Hawkins, Y. Choi, S.C. Huang, C.K. Hoh, M. Dahlbom, C. Schiepers, N. Satyamurthy, J. Barrio, M.E. Phelps. "Evaluation of the Skeletal Kinetics of <sup>18</sup>F-fluoride ion with PET," *J Nucl Med*, 1992; 33: pp. 633-642
- [6] R.E. Carson, Y. Yan, B. Chodowski, T.K. Yap, M.E. Daube-Witherspoon. "Precision and accuracy of regional radioactivity quantitation using maximum likelihood EM reconstruction algorithms." *IEEE Trans MI*, 1994; 13: pp. 526-537
- [7] E.U. Mumcuoglu, R.M. Leahy, S.R. Cherry. "Bayesian reconstruction of PET images: methodology and performance analysis." *Phys Med Biol*, 1996; 41: pp. 1777-1807